Error Propagation from Camera Motion to Epipolar Constraint

Xinquan Shen, Phil Palmer, Phil McLauchlan and Adrian Hilton
School of Electronic Engineering,
Information Technology & Mathematics
University of Surrey, Guildford, GU2 7XH, UK

Abstract

This work investigates the propagation of errors from the camera motion to the epipolar constraint. A relation between the perturbation of the motion parameters and the error in the epipolar constraint is derived. Based on this relation, the sensitivity of the motion parameters to the epipolar constraint is characterised, and a constraint on the allowed perturbation in a motion parameter in response to a threshold for the produced error in the epipolar constraint is determined. The presented error propagation model is useful to vision systems such as a mobile robot where the camera motion is provided by an odometry sensor. Experimental results on real images are presented.

1 Introduction

Projections of a scene point in two images can be related by the well-known epipolar constraint [1]. Assuming that the relative camera motion between the two images is not a pure rotation, the scene point and the two camera centres then define a plane (called the epipolar plane) which contains the images of the scene point and intersects with the two image planes in two lines (called the epipolar lines) (see Fig. 1). Thus, the projection of a scene point in one image must be on the epipolar line which can be determined from the projection of the scene in the other image. The epipolar constraint can be uniquely characterised by a fundamental matrix [3, 6] which is a 3×3 matrix encoding the information of the camera calibration and motion (see Section 2).

The epipolar constraint on two corresponding image points is often used to reduce the solution space of the matching problem [9, 5] which is itself crucial to vision tasks such as structure from motion [2, 12] and stereo vision [4, 1]. In this case, the fundamental matrix is computed from the camera calibration and motion which are supposed to be provided by the vision system[1]. Although the camera can be pre-calibrated using a sophisticated calibration algorithm, the camera motion between images may need to be determined at each time when the image is taken. Vision systems such as a mobile robot often have an odometry sensor which can be used to provide an estimate of the camera motion. The fundamental matrix directly derived from the camera motion provided by the odometry sensor is never perfect, because of the wheel slippage, backlash and friction. Without

[1]The epipolar geometry can also be estimated directly from two images, assuming the correspondence between image points in the two images is determined [13]. Here, we consider the inverse case that the epipolar geometry is needed for resolving the matching problem.

BMVC 2000 doi:10.5244/C.14.55

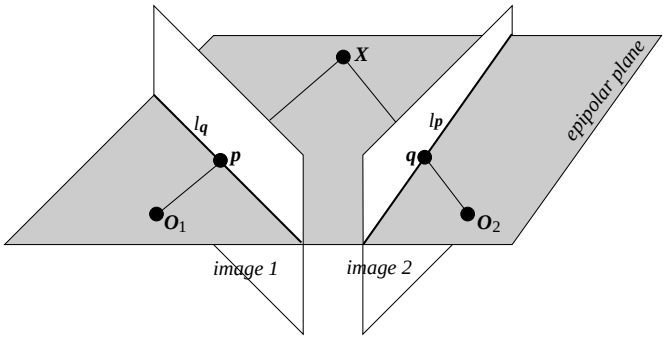

Figure 1: The epipolar constraint on two corresponding image points $\boldsymbol{p}$ and $\boldsymbol{q}$ which are the projection of the scene point $\boldsymbol{X}$. Points $\boldsymbol{p}$ and $\boldsymbol{q}$ are on the epipolar lines $l_{\boldsymbol{q}}$ and $l_{\boldsymbol{p}}$ respectively. The line $l_{\boldsymbol{p}}(l_{\boldsymbol{q}})$ is the intersection of the image plane 2(1) with the epiolar plane determined from camera positions $\boldsymbol{O}_1$ and $\boldsymbol{O}_2$, and the image point $\boldsymbol{p}(\boldsymbol{q})$.

considering the error in the epipolar constraint, the matching algorithm may reject correct candidates for matching or accept erroneous matchings. It is then important to know how much error is caused in the epipolar constraint due to the perturbation in the camera motion.

In this work, we investigate the propagation of errors from the camera motion to the epipolar constraint on two corresponding image points. The error in the epipolar constraint is simply characterised using the distance from an image point to the epipolar line derived from the corresponding image point in the other image. We first derive a relation between the perturbation of the motion parameters and the error in the epipolar constraint. Based on this relation, the sensitivity of a motion parameter to the epipolar constraint is characterised. We show that the effect of the motion perturbation on the epipolar constraint depends on the direction of the camera motion and the depth of the scene point. We then present a constraint on the allowed perturbation in a motion parameter in response to a specified error in the epipolar constraint. Thus, given a threshold for the allowed error in the epipolar constraint, the required accuracy in the measurement of a motion parameter can be determined, and vice versa.

The motivation of this work is in connection with the reconstruction of 3D environments using an autonomous mobile robot. The correct matching of feature points between successive images taken by the robot is important in order to obtain an accurate estimate of the 3D structure from a structure from motion algorithm [7]. In our matching algorithm [10], matching candidates are selected based on the epipolar constraint determined the camera motion estimated from the odometry of the robot. Since the range of the perturbation in odometry can often be empirically determined, the presented error propagation model then provides an extra constraint to enhance the robustness in determining matching candidates. Furthermore, the error model also provides a reference for balancing the required accuracy of the vision system in measuring the camera motion and the epipolar error which must be tolerated by applications on the system.

The rest of the paper is organised as follows. Section 2 describes the epipolar constraint characterised by the fundamental matrix which is expressed in terms of the camera calibration and motion. Section 3 discusses the error propagation from the camera motion to the epipolar constraint. The sensitivity of the motion parameters to the epipolar con-

straint is characterised. Section 4 presents a constraint on the allowed perturbation in a motion parameter in response to a specified error in the epipolar constraint. Experimental results are presented in section 5. Finally, section 6 is for conclusions.

2 Epipolar geometry

Projections of a scene point in two images can be related by the epipolar constraint which can be expressed as follows [3, 6]:

$$\boldsymbol{q}^T F \boldsymbol{p} = 0 \tag{1}$$

where, $\boldsymbol{p} = [x\, y\, 1]^T$ and $\boldsymbol{q} = [x'\, y'\, 1]^T$ represent projections of a scene point in the first and second images respectively, and F is a 3×3 matrix, called the fundamental matrix, which can be determined from the camera and motion parameters as follows:

$$F = C^{-T} R_2 [\boldsymbol{t}_1 - \boldsymbol{t}_2]_\times R_1^T C^{-1} \tag{2}$$

where, C is the calibration matrix describing the camera parameters, R_i and $\boldsymbol{t}_i$, $i = 1, 2$, are rotations and translations associated with the first and second images respectively, $[\boldsymbol{v}]_\times$ denotes the cross product of a 3×1 vector $\boldsymbol{v}$[2], and T denotes transpose operation on matrices and vectors.

Without loosing the generality, we assume $R_1 = I$ and $\boldsymbol{t}_1 = \boldsymbol{0}$, and use R and $\boldsymbol{t}$ to refer R_2 and $\boldsymbol{t}_2$ respectively. Equation (2) then becomes

$$F = C^{-T} R [-\boldsymbol{t}]_\times C^{-1} \tag{3}$$

The calibration matrix C can be expressed as follows (lens distortion is ignored):

$$C = \begin{bmatrix} f_x & 0 & x_0 \\ 0 & f_y & y_0 \\ 0 & 0 & 1 \end{bmatrix} \tag{4}$$

where, f_x and f_y are focal lengths in X-axis and Y-axis directions, and (x_0, y_0) is the image centre. The translation $\boldsymbol{t}$ is measured within a chosen world coordinate system, and expressed as $\boldsymbol{t} = [t_x\, t_y\, t_z]^T$, where, t_x, t_y, and t_z are translations in X, Y, and Z directions of the world coordinate system respectively. We use Euler angles to describe the rotation from the world coordinate system to the camera coordinate system [8]. The rotation transformation is characterised by first rotating the camera frame (at this time, it is aligned with the world frame) about Z-axis by an angle γ, then rotating the camera frame about its new Y-axis by an angle β, and finally rotating the camera frame about its current X-axis by an angle α. The physical meaning of rotation angles depends on the specific vision system. In our system, for example, α and β correspond to rotations in tilt and pan of the robot head respectively. The rotation matrix R then has the following form:

$$R = \begin{bmatrix} \cos\beta\cos\gamma & -\cos\beta\sin\gamma & \sin\gamma \\ \cos\alpha\sin\gamma + \sin\alpha\sin\beta\cos\gamma & \cos\alpha\cos\gamma - \sin\alpha\sin\beta\sin\gamma & -\sin\alpha\cos\beta \\ \sin\alpha\sin\gamma - \cos\alpha\sin\beta\cos\gamma & \sin\alpha\cos\gamma + \cos\alpha\sin\beta\sin\gamma & \cos\alpha\cos\beta \end{bmatrix} \tag{5}$$

[2] If $\boldsymbol{v} = [v_x\, v_y\, v_z]^T$, then

$$[\boldsymbol{v}]_\times = \begin{bmatrix} 0 & -v_z & v_y \\ v_z & 0 & -v_x \\ -v_y & v_x & 0 \end{bmatrix}$$

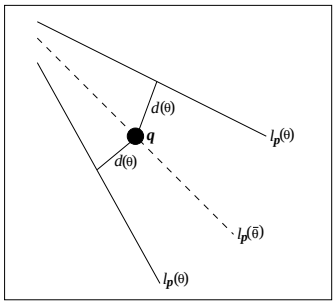

Figure 2: Characterisation of the error in the epipolar constraint on two corresponding point $\boldsymbol{p}$ and $\boldsymbol{q}$.

The epipolar constraint (1) indicates that the image point $\boldsymbol{q}$ is on a line $l_{\boldsymbol{p}}$: $au + bv + c = 0$ in image 2, where line parameters a, b and c are determined as follows:

$$\begin{bmatrix} a \\ b \\ c \end{bmatrix} = F\boldsymbol{p} = F \begin{bmatrix} x \\ y \\ 1 \end{bmatrix} \tag{6}$$

The line $l_{\boldsymbol{p}}$ is called the epipolar line associated with point $\boldsymbol{p}$. Geometrically, the epipolar line is the intersection of the image plane 2 with the epipolar plane which is determined from the image point $\boldsymbol{p}$ and two camera centres (see Fig. 1).

In practical situations, the camera calibration is often required to do once, and can be achieved off-line using a sophisticated algorithm. In the following discussion, we assume that the calibration matrix C is known, and the only error in the fundamental matrix is from the perturbation in the camera motion.

3 Error propagation

Let $\boldsymbol{\theta} = \begin{bmatrix} \boldsymbol{e} \\ \boldsymbol{t} \end{bmatrix}$, where, $\boldsymbol{e} = [\alpha\ \beta\ \gamma]^T$. Thus, $\boldsymbol{\theta}$ is a vector composed of all parameters describing the camera motion. The fundamental matrix F and the epipolar line $l_{\boldsymbol{p}}$ are then functions of the parameter vector $\boldsymbol{\theta}$, and will be referred as $F(\boldsymbol{\theta})$ and $l_{\boldsymbol{p}}(\boldsymbol{\theta})$ (with corresponding line parameters $a(\boldsymbol{\theta})$, $b(\boldsymbol{\theta})$ and $c(\boldsymbol{\theta})$) respectively. Obviously, when the parameter vector $\boldsymbol{\theta}$ is measured with errors, the epipolar constraint (1) may no longer be satisfied, i.e. the image point $\boldsymbol{q}$ may no longer be on the epipolar line $l_{\boldsymbol{p}}(\boldsymbol{\theta})$.

To characterise the error in the epipolar constraint on two corresponding points $\boldsymbol{p}$ and $\boldsymbol{q}$, we investigate the distance from the point $\boldsymbol{q}$ to the epipolar line $l_{\boldsymbol{p}}(\boldsymbol{\theta})$. Let $d(\boldsymbol{\theta})$ be the signed distance from $\boldsymbol{q}$ to $l_{\boldsymbol{p}}(\boldsymbol{\theta})$ (see Fig. 2). Then, $d(\boldsymbol{\theta})$ can be determined as follows:

$$d(\boldsymbol{\theta}) = \frac{\boldsymbol{q}^T F(\boldsymbol{\theta})\boldsymbol{p}}{[a^2(\boldsymbol{\theta}) + b^2(\boldsymbol{\theta})]^{1/2}} \tag{7}$$

The sign of $d(\boldsymbol{\theta})$ indicates which side the point $\boldsymbol{q}$ is located to the line $l_{\boldsymbol{p}}(\boldsymbol{\theta})$. Let $\bar{\boldsymbol{\theta}} = \begin{bmatrix} \bar{\boldsymbol{e}} \\ \bar{\boldsymbol{t}} \end{bmatrix}$ be the true value of $\boldsymbol{\theta}$. Then, $d(\bar{\boldsymbol{\theta}}) = 0$. Assuming that $\boldsymbol{\theta}$ varies around $\bar{\boldsymbol{\theta}}$ within

a small neighbourhood, we can approximate $d(\boldsymbol{\theta})$ by expanding it at $\bar{\boldsymbol{\theta}}$ till the first order, i.e.

$$d(\boldsymbol{\theta}) \approx \sum_i \frac{\partial d(\bar{\boldsymbol{\theta}})}{\partial \theta_i} \delta\theta_i \tag{8}$$

where θ_i is the ith component of the parameter vector $\boldsymbol{\theta}$ and $\delta\theta_i = \theta_i - \bar{\theta}$. From the equation (7), we have

$$\frac{\partial d(\bar{\boldsymbol{\theta}})}{\partial \theta_i} = \frac{\boldsymbol{q}^T \frac{\partial F(\bar{\boldsymbol{\theta}})}{\partial \theta_i} \boldsymbol{p}}{[a^2(\bar{\boldsymbol{\theta}}) + b^2(\bar{\boldsymbol{\theta}})]^{1/2}} \tag{9}$$

For a specific motion parameter θ_i, $\frac{\partial F(\bar{\boldsymbol{\theta}})}{\partial \theta_i}$ can be determined from the equation (3). For example, for the rotation parameter α,

$$\frac{\partial F(\bar{\boldsymbol{\theta}})}{\partial \alpha} = C^{-T} \frac{\partial R}{\partial \alpha} [-\boldsymbol{t}]_\times C^{-1} \Big|_{\bar{\boldsymbol{\theta}}} \tag{10}$$

Let $\delta d_{\theta_i} = \frac{\partial d(\bar{\boldsymbol{\theta}})}{\partial \theta_i} \delta\theta_i$. Then, δd_{θ_i} characterises the induced epipolar error due the perturbation of the parameter θ_i. Therefore, $d(\boldsymbol{\theta})$ can be evaluated as the sum of errors produced from perturbations of each motion parameter.

For two corresponding image points, the value of $d(\boldsymbol{\theta})$ is, however, dependent upon the camera motion. The motion perturbation in the translation direction has no effect on the epipolar constraint. Assume

$$\boldsymbol{\theta} = \begin{bmatrix} \bar{\boldsymbol{e}} \\ \bar{\boldsymbol{t}} + \lambda \boldsymbol{n} \end{bmatrix} \tag{11}$$

where, $\boldsymbol{n} = \bar{\boldsymbol{t}}/\|\bar{\boldsymbol{t}}\|$ is the direction of the camera translation $\bar{\boldsymbol{t}}$, and λ is a constant. Obviously, $\boldsymbol{\theta}$ differs from $\bar{\boldsymbol{\theta}}$ with a perturbation of the magnitude λ in the camera translation $\bar{\boldsymbol{t}}$. Substituting the components of $\boldsymbol{\theta}$ into the equation (3), we have $F(\boldsymbol{\theta}) = (1 + \lambda/\|\bar{\boldsymbol{t}}\|)\, F(\bar{\boldsymbol{\theta}})$ which then leads to $d(\boldsymbol{\theta}) = \pm d(\bar{\boldsymbol{\theta}}) = 0$. This means that epipolar lines are invariant to the motion perturbation along the camera translation only.

In the general case, $d(\boldsymbol{\theta})$ or δd_{θ_i} needs to be evaluated in order to examine the effect of motion parameters on the epipolar constraint. Direct evaluation of the term $\frac{\partial d(\bar{\boldsymbol{\theta}})}{\partial \theta_i}$ requires the knowledge of the true camera motion $\bar{\boldsymbol{\theta}}$. In practical situation, we may only know an estimate of the $\bar{\boldsymbol{\theta}}$, $\hat{\boldsymbol{\theta}}$. For example, when images are captured using a mobile robot, the odometry of the robot can be used to provide an estimate of the true camera motion. Provided $\hat{\boldsymbol{\theta}}$ is within a small neighbourhood of $\bar{\boldsymbol{\theta}}$, then $\frac{\partial d(\bar{\boldsymbol{\theta}})}{\partial \theta_i} = \frac{\partial d(\hat{\boldsymbol{\theta}})}{\partial \theta_i}$ to the first order. Thus, for a typical measurement error $\delta\boldsymbol{\theta}$, the induced error in the epipolar constraint can be estimated.

The induced error in the epipolar constraint also depends upon the depth of the corresponding scene point to the image plane. Assume $\boldsymbol{p}$ and $\boldsymbol{q}$ are images of a scene point $\boldsymbol{X} = [X\ Y\ Z]^T$ in space. Then $\boldsymbol{p}$ and $\boldsymbol{q}$ can be written as follows:

$$\begin{aligned} \xi_1 \boldsymbol{p} &= C\boldsymbol{X} \\ \xi_2 \boldsymbol{q} &= CR\boldsymbol{X} - CR\boldsymbol{t} \end{aligned} \tag{12}$$

where, ξ_1 and ξ_2 are distances (depths) from the point $\boldsymbol{X}$ to image planes 1 and 2 respectively. Substituting above equations into (7), we can find that the error $|d(\boldsymbol{\theta})|$ decreases

as the increase of the depth ξ_2, for a given scene point $\boldsymbol{X}$. Thus, for a given measurement error $\delta\boldsymbol{\theta}$, image points corresponding to front scene points tend to have a larger error in the epipolar constraint than those corresponding to scene points on the back.

Assume that the error in the measurement of the motion parameter θ_i is random and has a Gaussian distribution with zero mean and variance σ_i^2, i.e. $\delta\theta_i$ is a random variable with a Gaussian distribution $N(0, \sigma_i^2)$. Also, assume that each motion parameter is independently estimated by the vision system, i.e. $\delta\theta_i$ and $\delta\theta_j$, $i \neq j$, are independent. It then follows that $d(\boldsymbol{\theta})$ is also random and has a Gaussian distribution $N(0, \sigma^2)$, where,

$$\sigma^2 = \sum_i \left(\frac{\partial d(\bar{\boldsymbol{\theta}})}{\partial \theta_i} \sigma_i \right)^2 \tag{13}$$

The value of σ then characterises the sensitivity of the epipolar constraint on two corresponding image points to perturbations from all motion parameters. The larger the value of σ is, the more sensitive the epipolar constraint is.

4 Bound of errors

Based on the error propagation discussed in previous sections, we can also relate the accuracy in the camera motion to the accuracy in the epipolar constraint. Thus, we can derive a constraint on the bound of errors in the camera motion and the epipolar constraint.

According to the equation (8), given a measurement error $\delta\boldsymbol{\theta}$, we can estimated the induced error in the epipolar constraint. Conversely, given a threshold for the allowed error in δd_{θ_i} produced due to the perturbation in motion parameter θ_i, we can determine the required accuracy in the measurement of the parameter θ_i. Assuming that D_i is a threshold for the allowed maximum error in δd_{θ_i}, the required accuracy in the measurement of θ_i can be correspondingly determined from the constraint $|\frac{\partial d(\bar{\boldsymbol{\theta}})}{\partial \theta_i} \delta\theta_i| \leq D_i$. This constraint on the bound of errors is often useful to a vision system which has a sensor for the camera motion. It provides a relation for balancing the error which must be tolerated by applications based on the epipolar constraint and the accuracy of the system (e.g. the odometry of a mobile robot) for estimating the camera motion.

5 Experimental results

Experiments have been applied to pairs of images captured using a mobile robot mounted with a single CCD camera. The camera coordinate system is defined so that its Z-axis is aligned with the optical axis of the camera. The motion of the camera is determined by a translation within the world coordinate system which is defined with a known relation to the camera frame associated with the first image, and a rotation in tilt and pan angles which correspond to the Euler angles α and β respectively (see Section 2). The translation is measured in centimetres while the rotation is measured in degrees. The camera is calibrated using a robust calibration algorithm [11]. The odometry of the robot is used to provide an estimate of the camera motion to evaluate the effect of the motion parameters on the epipolar constraint.

For each pair of images, a set of corresponding points are chosen by applying an automatic junction detection and matching operation [10] and then removing outliers. For

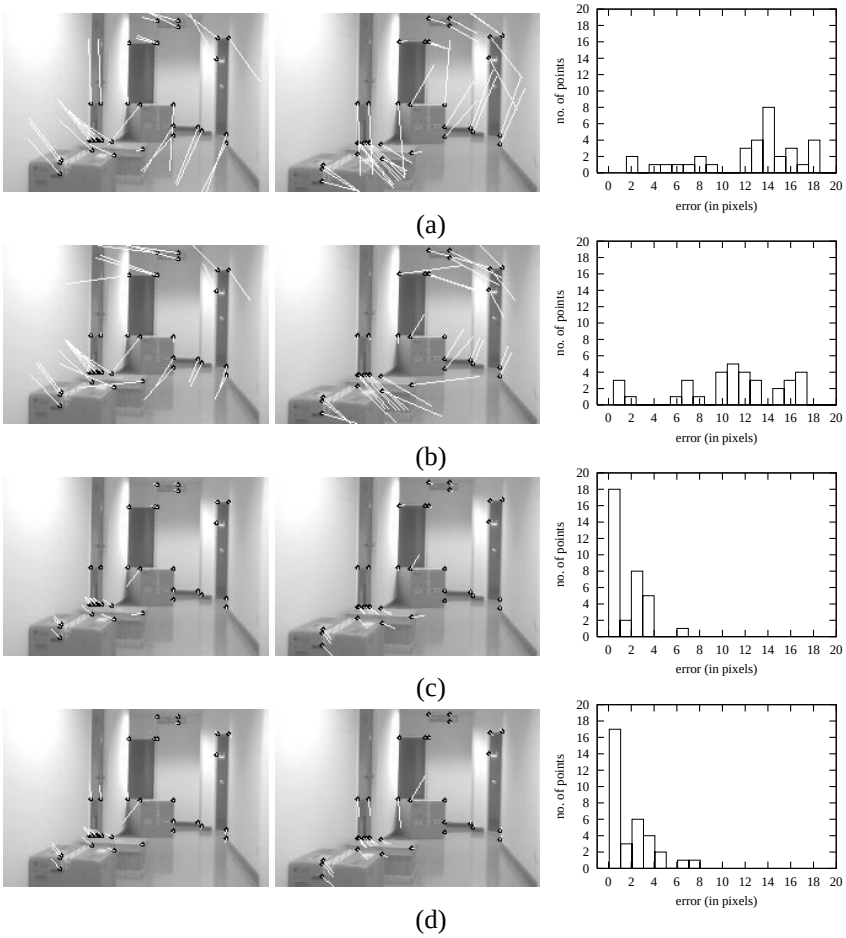

Figure 3: Experimental result on a pair of images in a sequence captured by a mobile robot moving along a corridor. (a), (b), (c) and (d) present the epipolar errors caused by the perturbation in tilt angle α, pan angle β, translation t_x and translation t_y respectively. In each case, the left two images show the epipolar error at each pair of corresponding points, while the right graph shows the distribution of errors at points in the first image.

each pair of corresponding points, the epipolar errors δd_{θ_i} produced from the perturbation of each motion parameter are evaluated. The value of $\delta\theta_i$ is taken as 1 degree for rotation parameters, and 1cm for translation parameters. Histograms describing the distribution of δd_{θ_i} for all chosen corresponding points in the image are also computed.

Fig. 3 shows the experimental result on a pair of two images in a sequence taken as the robot moves along a corridor. Each image has a resolution of 720×484 pixels. The world coordinate system is defined to be aligned with the camera frame associated with the first image. The camera motion involves a single translation along the Z-axis of the world coordinate system. According to the discussion in Section 3, the perturbation in translation parameter t_z then has no effect on the epipolar constraint. This means that, in this case, the accuracy in measuring t_z is not important to the epipolar constraint. Fig. 3a,

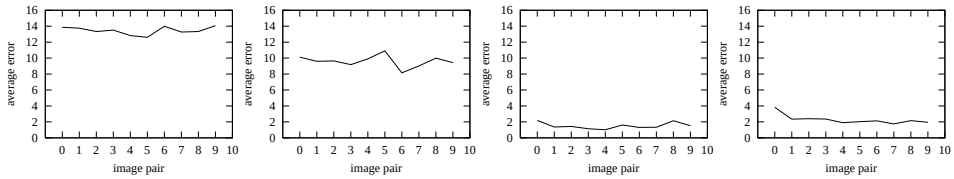

Figure 4: Average epipolar errors in 10 successive pairs of images in the corridor sequence. (a), (b), (c) and (d) show the average errors caused by the perturbation in tilt angle α, pan angle β, translation t_x and translation t_y respectively.

Fig. 3b, Fig. 3c and Fig. 3d show the epipolar errors produced from the perturbation in tilt angle α, pan angle β, translation t_x and translation t_y respectively. In each case, the left two images show the epipolar error at each pair of corresponding points. The error is represented as a vector originated from the point of interest and pointed towards the epipolar line derived from the corresponding point in the other image[3]. A large vector indicates a large error in the epipolar constraint. The distribution of errors at points in the first image is shown in the right graph. It can be seen that, in this example, a 1° error in rotation parameters α and β will cause much more error in the epipolar constraint than a 1cm error in translation parameters t_x and t_y. For most of points, epipolar errors caused by translations are less than 5 pixels, while epipolar errors caused by rotations are around 15 pixels.

To investigate the consistency in the sensitivity of a motion parameter within an image sequence, we also compute the average of epipolar errors on all corresponding points in each successive pair of images in the sequence. Fig. 4 presents average epipolar errors in 10 successive pairs of images in the corridor sequence. Fig. 4(a), Fig. 4(b), Fig. 4(c) and Fig. 4(d) show the average errors caused by the perturbation in tilt angle α, pan angle β, translation t_x and translation t_y respectively. It can be seen that, given a 1° error in rotations and 1cm error in translations, rotation parameters α and β are consistently more sensitive to the epipolar constraint than translation parameters t_x and t_y. For the perturbation in translations, the produced error is, in average, about 2 pixels. Approximately, an accuracy of a perturbation less than 0.14° in tilt and 0.2° in pan is required in order to ensure the produced epipolar error is within 2 pixels.

Fig. 5 shows the result of an experiment applied to a pair of two images in a sequence taken as the robot moves across a lab. Each image has a resolution of 720×576 pixels. The camera involves a single translation. The initial camera configuration is calibrated, and the world coordinate system is defined so that its Z-axis is aligned with the direction of the camera translation. Thus, the perturbation in translation parameter t_z has no effect on the epipolar constraint. Fig. 5a, Fig. 5b, Fig. 5c and Fig. 5d show the the epipolar errors produced from the perturbation in tilt angle α, pan angle β, translation t_x and translation t_y respectively. In each case, the left two images show the error at each pair of corresponding points, while the right graph shows the distribution of errors at points in the first image. It can be seen that, in this example, the perturbation in the tilt angle α will cause much more error in the epipolar constraint than the perturbation in the pan angle β. This is not surprising since the perturbation in the tilt angle is in the direction vertical

[3]Vectors are properly scaled in order to display them in images. Here, the same scale factor is used for all cases. The effect on different cases can then be compared based on the length of vectors.

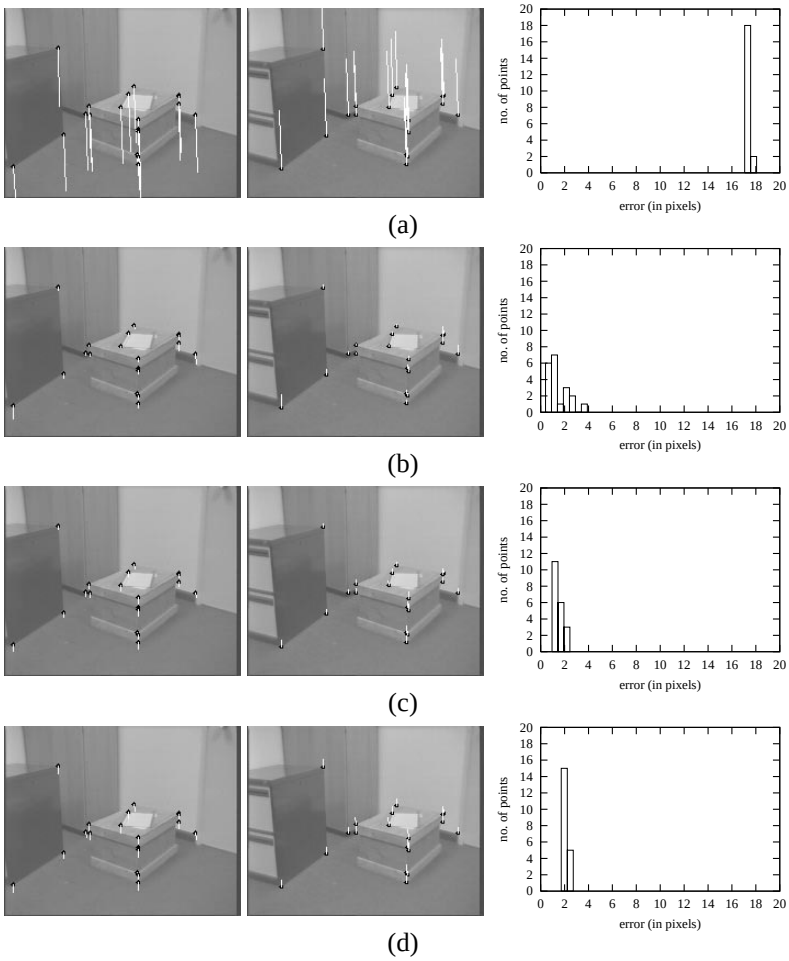

Figure 5: Experimental result on a pair of images in a sequence captured by a mobile robot moving across a lab. (a), (b), (c) and (d) present the epipolar errors caused by the perturbation in tilt angle α, pan angle β, translation t_x and translation t_y respectively. In each case, the left two images show the epipolar error at each pair of corresponding points, while the right graph shows the distribution of errors at points in the first image.

to the direction of the camera motion while the perturbation in the pan angle is in the direction along the camera motion. Errors caused by a 1cm perturbation in translations t_x and t_y are less than 3 pixels.

6 Conclusion

We have discussed the propagation of errors from the camera motion to the epipolar constraint. We have derived a relation between the perturbation in the camera motion and the error in the epipolar constraint. We have shown that the error propagation depends on the direction of the camera motion and the depth of the scene point. The effect of a

motion parameter on the epipolar constraint has been characterised. A constraint on the allowed perturbation in a motion parameter in response to a specified error in the epipolar constraint is also presented. Experiments on real images show that a rotation perturbation vertical to the direction of the camera motion is more sensitive to the epipolar constraint than a perturbation in translations. Approximately, an accuracy of a perturbation less than 0.1° in rotations is required in order to ensure that the produced epipolar error is at the similar level as the one produced by a 1cm error in translations.

The presented model for error propagation is useful to vision systems such as a mobile robot where the camera motion is provided by an odometry sensor. It provides a reference for balancing the required accuracy of the vision system in measuring the camera motion and the epipolar error which must be tolerated by applications on the system. It also can be used to derive a constraint to refine the solution space for the matching problem. Experimental results have been presented on real images.

References

[1] N. Ayache. *Artificial Vision for Mobile Robots: Stereo Vision and Multisensory Perception*. MIT press, Cambridge, Massachusetts, 1991.

[2] R. C. Bolles, H. H. Baker, and D. H. Marimont. Epipolar-plane Image-analysis — An Approach to Determining Structure from Motion. *International Journal of Computer Vision*, 1(1):7–55, 1987.

[3] Oliver Faugeras. *Three Dimensional Computer Vision*. The MIT Press, 1993.

[4] W. Grimson. Computational Experiments with a Feature Based Stereo Algorithm. *IEEE Transactions on Pattern Analysis and Machine Intelligence*, 7(1):17–34, January 85.

[5] X. Hu and N. Ahuja. Matching Point Features with Ordered Geometric, Rigidity, and Disparity Constraint. *IEEE Transactions on Pattern Analysis and Machine Intelligence*, 16(10):1041–1049, October 1994.

[6] Q. T. Luong and O. D. Faugeras. The Fundamental Matrix: Theory, Algorithms, and Stability Analysis . *International Journal of Computer Vision*, 17(1):43–75, 1996.

[7] P. F. McLauchlan, X. Shen, A. Manessis, P. Palmer, and A. Hilton. Surface-Based Structure-from-Motion Using Feature Groupings. In *Asian Conference on Computer Vision 2000*, volume 2, pages 699–705, Taipei, Taiwan, January 2000.

[8] R. M. Murray, Z. Li, and A. S. Sastry. *A Mathematical Introduction to Robotic Manipulation*. CRC Press, Boca Raton, New York, 1994.

[9] M. D. Pritt. Image Registration with Use of the Epipolar Constraint for Parallel Projections. *Journal of the Optical Society of America A — Optics Image Science and Vision*, 10(10):2187–2192, 1993.

[10] X. Shen and P. Plamer. Uncertainty Propagation and the Matching of Junctions as Feature Groupings. Submitted to IEEE Transactions on Pattern Analysis and Machine Intelligence.

[11] T. Wang, P. F. McLauchlan, P. Palmer, and R. Patenall. An Accurate Camera Calibration Approach Based on a Sequence of Images. Technical Report VSSP-TR-1/2000, University of Surrey.

[12] J. Weng, T. S. Huang, and N. Ahuja. *Motion and Structure from Image Sequences.* Springer-Verlag, Berlin, 1993.

[13] Z. Zhang. Determining the Epipolar Geometry and its Uncertainty: A Review. *International Journal of Computer Vision*, 27(2):161–195, 1998.